processes

MDPI

Review

Bayesian Network Modeling for Risk-Based Water Quality Decisions with Sparse Data: Case Study of the Kiso River

Ola Mohamed [1,*] and Nagahisa Hirayama [2]

[1] Graduate School of Environmental Studies, Nagoya University, Chikusa, Nagoya 464-8601, Japan
[2] Disaster Mitigation Research Centre, Nagoya University, Chikusa, Nagoya 464-8601, Japan
* Correspondence: mohamed.ola.mamoun.ahmed.u6@s.mail.nagoya-u.ac.jp

Abstract

The study aims to explore the causal relationships among climate, hydrological, and water quality variables in the Kiso River Basin, Japan, using a discrete Bayesian Network (BN) model. The BN was developed to represent probabilistic dependencies between climate factors (rainfall, air temperature), hydrological conditions (river flow levels), and water quality indicators (pH, dissolved oxygen [DO], electrical conductivity, ammonia, turbidity, organic pollution, and water temperature). The model used hourly monitoring data collected between 2016 and 2023, and the continuous variables were discretized based on national environmental thresholds to evaluate exceedance probabilities under different hydro-climatic scenarios. Results showed that air temperature strongly influenced water temperature, with a stabilizing effect under constant flow conditions. Rainfall and river flow were key drivers of turbidity; heavy rainfall and high flow increased the probability of exceeding turbidity thresholds by nearly 80%. Elevated ammonia levels during heavy rainfall and low temperatures reflected runoff and limited nitrification processes. Electrical conductivity decreased during high flows due to dilution, while dissolved oxygen was affected by low flows, turbidity, and temperature. As static BNs cannot model temporal dynamics, supplementary cross-correlation analyses were conducted to assess short-term responses among variables, revealing that most water quality parameters respond within ±24 h to changes in hydrological conditions. This study demonstrates that discrete BNs can effectively translate long-term monitoring data into practical, decision-relevant risk assessments to support adaptive water quality management in dynamic river systems.

Keywords: Bayesian Networks (BNs); water quality assessment; causal relationships; Japan; Kiso River

check for updates

Academic Editor: Marcus Vinicius Tres

Received: 15 October 2025
Revised: 4 November 2025
Accepted: 5 November 2025
Published: 10 November 2025

Citation: Mohamed, O.; Hirayama, N. Bayesian Network Modeling for Risk-Based Water Quality Decisions with Sparse Data: Case Study of the Kiso River. *Processes* **2025**, *13*, 3636. https://doi.org/10.3390/pr13113636

Copyright: © 2025 by the authors. Licensee MDPI, Basel, Switzerland. This article is an open access article distributed under the terms and conditions of the Creative Commons Attribution (CC BY) license (https://creativecommons.org/licenses/by/4.0/).

1. Introduction

Climatic, hydrological, and anthropogenic factors significantly influence river water quality, both directly and indirectly [1–8]. These complex interactions introduce substantial uncertainty and variability in climatic and hydrological processes [9]. Furthermore, this variability justifies the use of probabilistic modeling frameworks, such as Bayesian Networks, to capture uncertain dependencies [10]. To address these uncertainties, several probabilistic approaches have been developed in water quality modeling. These include Monte Carlo Methods, Generalized Likelihood Uncertainty Estimation (GLUE), Sensitivity Analysis, Bootstrap Methods, Probabilistic Neural Networks, and Causal Inference and Time-Frequency Analysis [11–17]. Uncertainty analysis is therefore critical for effective modeling and decision-making. Table 1 presents a comparison of the commonly used

probabilistic uncertainty analysis methods in water quality modeling. Table 1 displays commonly used problematic models for water quality modeling and highlights Bayesian Networks' (BNs) advantages in combining causal modeling with probabilistic reasoning.

Recent studies have applied BNs to water quality modeling. For example, an earlier study used BN to predict the concentration of trihalomethanes in drinking water systems, showcasing how BN captures multivariable interactions [18]. Similarly, Wei et al. (2024) utilized a BN model for phosphorus source attribution at the subwatershed scale [19]. Consequently, BNs are particularly more capable of research involving sparse, incomplete, or uncertain datasets [20,21].

Recent applications of Bayesian Networks (BNs) have primarily focused on localized conditions or specific pollutants, limiting the generalizability of findings due to narrow spatial coverage and simplified variable representation [22–30]. Building on these studies, the present research integrates multiple physicochemical water quality parameters with hydro-climatic variables, rainfall, river flow, and air temperature, using high-frequency (hourly) data collected over seven years (2016–2023). This approach enables a comprehensive, data-driven assessment of interactions among climatic, hydrological, and water quality factors in the Kiso River Basin.

The study aims to:

1 Quantify the influence of seasonality, rainfall, temperature, and river flow on key water quality parameters, including turbidity, electrical conductivity, pH, dissolved oxygen, ammonia, and organic pollution.
2 Capture the causal dependencies among these indicators by developing and parameterizing a discrete Bayesian Network.
3 Assess water quality risks under varying environmental conditions through probabilistic analysis.

This data-driven BN framework provides probabilistic insights even when datasets are incomplete and translates results into actionable thresholds to support operational decision-making for adaptive water quality management.

The model employs high-frequency hourly monitoring data over a seven-year period (2016–2023), which captures fine-scale temporal dynamics in the Kiso River. In addition, this data-driven framework delivers probabilistic insights even when datasets are incomplete and translates these insights into actionable thresholds that support operational decision-making for water quality management.

Table 1. Comparison of probabilistic uncertainty analysis methods in water quality modeling.

Method	Insights	References
Markov Chain Monte Carlo (MCMC)	Stochastic simulation: powerful in handling uncertainty but does not infer causality.	[31,32]
GLUE	Likelihood-based probabilistic method using behavioral thresholds.	[33–35]
Sensitivity Analysis	Useful for identifying key variables.	[36]
Bootstrap Methods	A data-driven resampling method for quantifying empirical uncertainty.	[37]
Probabilistic Neural Networks	Machine learning, able to model probabilistic classification.	[38]
Bayesian Networks (BNs)	Model probabilistic causal relationships.	[39]

As summarized in Table 1, Bayesian Networks offer a distinct advantage in representing causal dependencies and integrating both data and expert knowledge. However, they

are also sensitive to the assumed network structure and require careful discretization to avoid loss of information. These strengths and limitations guided the model development and validation strategy in this study.

While previous BN studies have demonstrated strong predictive capability, many have relied on sparse temporal data or assumed fixed causal structures. These limitations can constrain model transferability. By employing a long-term, high-resolution dataset and incorporating hydrological process knowledge into network design, this study improves both causal interpretability and robustness.

2. Study Area and Data Description

The study area is the Kiso River, one of the "Kiso Three Rivers," which also include the Nagara River and the Ibi River. The river originates from the Kiso Mountains of Nagano Prefecture and flows approximately 229 km, with a catchment area of 5275 km^2. Figure 1 shows the Kiso River Watershed map (source: Ministry of Land, Infrastructure, Transport and Tourism), providing the geographical context for the study area. The Kiso River plays a critical role in municipal, agricultural, and industrial sectors. The water quality status, including turbidity (NTU), electrical conductivity (μS/cm), pH, dissolved oxygen (mg/L), ammonia (mg/L), and organic pollution (mg/L), was provided by the City of Nagoya's Water and Sewerage Bureau. These parameters were selected primarily based on their availability, consistency, and reliability. Additionally, these parameters are crucial for defining pollution risks [40–42].

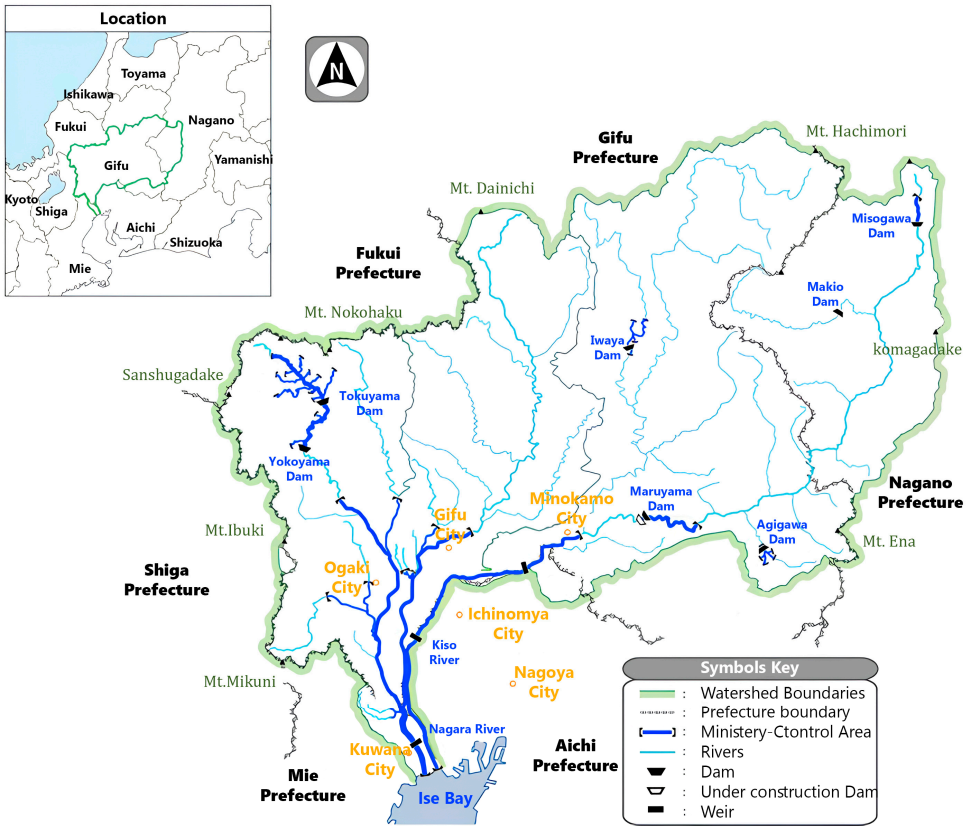


Figure 1. Kiso River Watershed map (sourced for translation from: Ministry of Land, Infrastructure, Transport and Tourism).

The study prioritizes modeling conditional dependencies among hydro-climatic and water quality variables rather than detailed spatial mapping, as the objective is to understand system-level interactions rather than spatial distribution patterns. The study

used measurements from two hydrological stations located in Gifu Imato (35.4358° N, 137.0333° E) and Nagano Momoyama (35.7617° N, 137.7039° E), to assess river flow levels, rainfall, and temperature dynamics. Although only two hydrological stations were used, they were strategically located to represent upstream and downstream sections of the Kiso River. Therefore, while spatial variability is simplified, the selected sites capture major hydrological gradients relevant to system-scale interpretation.

Hourly averages were calculated for both stations to capture short-term fluctuations and were incorporated into the analysis to examine their influence on water quality parameters. Seasonal effects were represented implicitly through the inclusion of temperature and rainfall variables, while no daily aggregation was applied to preserve fine-scale dynamics essential for causal dependency modeling. Representative data for rainfall and river flow were obtained from the Japan Ministry of Land, Infrastructure, Transport, and Tourism. Air temperature (°C) data from the nearest monitoring stations were obtained from the Japan Meteorological Agency, using monitoring hourly data collected between 2016 and 2023.

Preprocessing of Data

Data integration was conducted using the Extract–Transform–Load (ETL) processes. Raw data were collected from the mentioned sources, standardized into a uniform format, and combined into a single dataset. The integrated dataset contained missing values and outliers, which could have compromised the accuracy and validity of the analysis. To address these issues, systematic preprocessing steps were applied. Outlier detection was performed on rainfall and river flow measurements, with negative values replaced using mean imputation. Missing water quality data for November 2020 were addressed through seasonal imputation, using periodic fluctuations observed in 2016–2019. These preprocessing procedures ensured the integrity and reliability of the dataset for subsequent analysis.

3. Bayesian Network (BN)

To quantify the influence of climatic and hydrological drivers on water quality parameters, the model employed conditional probability distributions (CPDs) between variables. In this framework, nodes correspond to variables and edges represent direct causal influences [25–27,29]. The variables, represented as $X = \{X1,X2,\ldots,Xn\}$, are structured into a direct acyclic graph (DAG) that explicitly captures their conditional dependencies. This distribution can be expressed as:

$$P\,(X1, X2, \ldots, Xn) = \prod_{i=1}^{n} P\,(Xi|Pa(Xi)) \quad (1)$$

where $Pa(Xi)$ represent the set of parent nodes of Xi in the DAG. Each variable (Xi) is assigned to a hydrological, climatic, or water quality parameter in the study. Parent–child relationships were defined according to hydrological and ecological processes, which are defined and visualized in Section 3.2.

The Bayesian Network was implemented in Python 3.11. using the pgmpy library, which was used for the estimation of conditional probability distributions (CPDs) directly from the observed dataset [43].

3.1. Data Preparation and Discretization

Water quality and hydrological parameters were collected from representative monitoring stations between 2016 and 2023. Rainfall and river flow data were obtained from the Ministry of Land, Infrastructure, Transport, and Tourism (MLIT), air temperature data from the Japan Meteorological Agency (JMA), and water quality parameters, including turbidity, electrical conductivity, pH, dissolved oxygen, ammonia, and organic pollution, were provided by the City of Nagoya Water and Sewerage Bureau.

The key variables and their corresponding parameters, units, sources, and measurement frequencies are summarized in Table 2:

Table 2. Variables used in Bayesian network modeling.

Variable	Parameter	Unit	Source	Frequency
X1	Rainfall	mm/hour	MLIT	Hourly
X2	River Flow	m	MLIT	Hourly
X3	Air Temperature	°C	JMA	Hourly
X4	Water Temperature	°C	City of Nagoya Water and Sewerage Bureau	Hourly
X5	Dissolved Oxygen (DO)	mg/L	City of Nagoya Water and Sewerage Bureau	Hourly
X6	pH	–	City of Nagoya Water and Sewerage Bureau	Hourly
X7	Electrical Conductivity (EC)	µS/cm	City of Nagoya Water and Sewerage Bureau	Hourly
X8	Turbidity	NTU	City of Nagoya Water and Sewerage Bureau	Hourly
X9	Ammonia (NH_3–N)	mg/L	City of Nagoya Water and Sewerage Bureau	Hourly
X10	Organic Pollution	mg/L	City of Nagoya Water and Sewerage Bureau	Hourly

To model continuous variables with a discrete BN, all parameters were discretized based on environmental thresholds or government standards.

3.1.1. Hydrological and Climatic Data

Rainfall (mm/hour)

The bin thresholds for rainfall are based on the Japan Meteorological Agency's "Forecast Terminology" in Table 3.

Table 3. Rainfall categorized bins.

Hourly Rainfall (mm/hour)	Category	Explanation
0.0	No Rain	No measurable precipitation.
>0 to ≤10	Light Rain	Gentle rainfall, possibly including drizzle or intermittent rain. Not enough to cause flooding.
>10 to ≤30	Moderate Rain	Rain strong enough to wet roads quickly and potentially impact visibility.
>30	Heavy Rain	May cause localized flooding, especially in poor drainage areas.

Source: Japan Meteorological Agency.

River Flow (m)

According to the official Nagano City Flood Hazard Map of the Kiso River, water levels exceeding 6 m pose a serious flood risk and may necessitate evacuation orders. In this study, river flow was categorized into the following thresholds: low flow (under typical conditions), moderate flow (indicating elevated water levels requiring monitoring), and high flow (representing severe flood potential) (Table 4).

Table 4. River flow categorized bins.

Water Level (m)	Category	Note
<7.5	Low	Typical river water level under normal conditions.
>7.5 to ≤10	Medium	
>10	High	Serious flood risk; evacuation orders are likely issued.

Air Temperature (°C)

Based on the average monthly temperatures from the Japan Meteorological Agency (JMA) for Nagano City, where the air temperature values were obtained from 2016 to 2023, the three bins are defined in Table 5.

Table 5. Air temperature categorized bins.

Air Temperature (°C)	Bins	Description
<15 °C	Cold	Typically observed during winter or early spring. Cooler conditions with reduced biological activity.
15–25 °C	Moderate	Common in spring, autumn, and early summer. Comfortable temperatures, supporting stable ecosystems.
>25 °C	Warm/Hot	Seen during the summer months. Higher temperatures can increase evaporation and stress on water systems.

3.1.2. Water Quality Data

An exploratory analysis of the water quality data revealed that some parameters met Japan's environmental quality standards for water pollution (Figure 2) [44]. To improve the BN's interpretability, all variables were discretized into meaningful categorical bins. This was defined based on government thresholds [45] (Table 6).

Table 6. Water quality parameters observed ranges, suggested bins, and government thresholds.

Parameter	Observed	Bins	Government Thresholds/Typical Values
pH	4.0–8.14	Acidic (<6.5) Neutral (6.5–7.5) Alkaline (>7.5)	6.5–8.5
Dissolved oxygen (DO) (mg/L)	0.0–15.9	Low (<4) Moderate (4–8) High (>8)	≥7.5 mg/L
Electrical conductivity (μS/cm)	0.0–117.3	Very Low (<20) Low (20–50) Moderate (>50)	Typically, <300–500 μS/cm
Ammonia (NH_3-N) (mg/L)	0.0–0.03	Very Low (<0.005) Low (0.005–0.02) Moderate (>0.02)	≤0.02 mg/L
Turbidity (NTU)	0.0–964.2	Clear (≤5) Moderate (5–50) High (>50)	≤5 NTU

Table 6. *Cont.*

Parameter	Observed	Bins	Government Thresholds/Typical Values
Organic pollution (mg/L)	0.0–0.5	Very Low (≤0.1) Low (0.1–0.3) Moderate (>0.3)	Not explicitly regulated by the government threshold but divided based on actual data
Water temperature (°C)	0.0–26.9	Cold (<5) Cool (5–20) Warm (>20)	Seasonal range approx. 5–20 °C

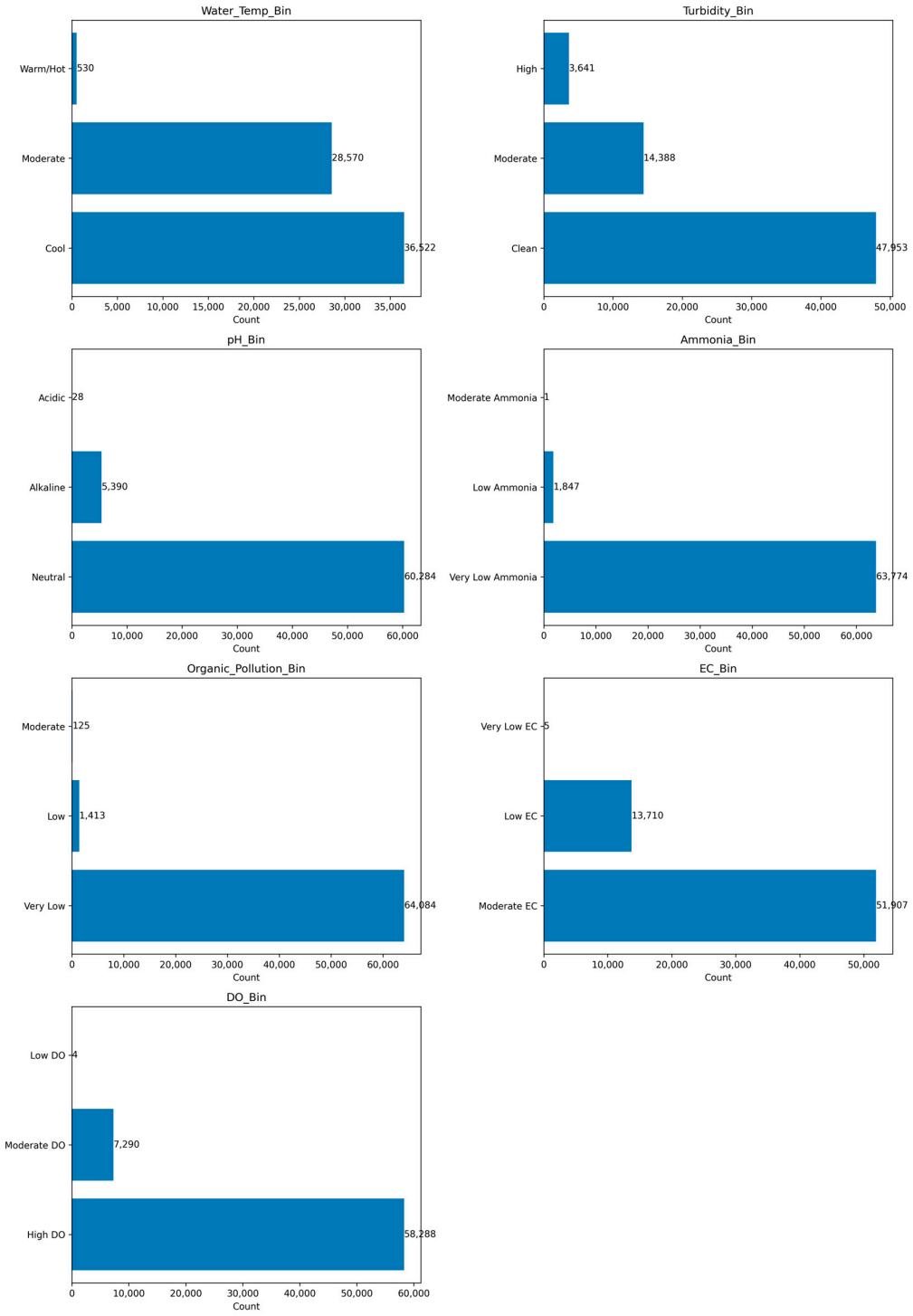


Figure 2. Distribution of water quality parameters.

3.2. BN Structure and Causal Relationships

The BN structure (Figure 3) illustrates the causal relationships between water quality parameters and major drivers (rainfall, river flow, air temperature, seasonality, water temperature). These links were established based on previous studies' findings.

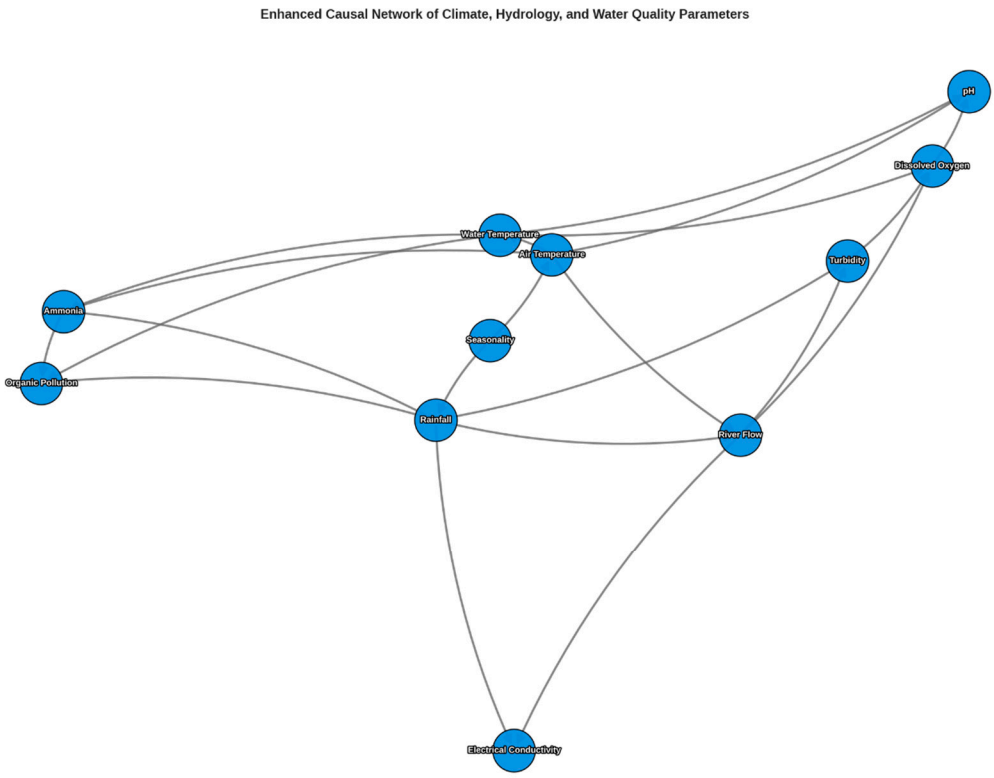


Figure 3. BN model.

Seasonality influences hydrological and climatic conditions, including rainfall and temperature, which vary regionally [46,47]. Furthermore, rainfall is the primary driver of increased river flow, affecting water levels and surface runoff, which in turn lead to changes in turbidity, electrical conductivity, and dissolved oxygen [48–50]. Ammonia is influenced not only by runoff and pollutant transport mechanisms [51] but also by water temperature through microbial activities, specifically those of ammonia-oxidizing bacteria (AOB) and ammonia-oxidizing archaea (AOA) [52]. Ammonia loading, on the other hand, is a key factor affecting organic pollution, which subsequently influences pH [53].

Turbidity affects DO levels by altering light penetration, which is essential for photosynthetic oxygen production [54].

3.3. Parameter Learning Using Maximum Likelihood Estimation (MLE)

The study used MLE to estimate the CPDs for each node under specific parent node(s). The full dataset was randomly split into 80% for training and 20% for testing to calculate the relative frequencies of the state combinations [55]. A similar approach was also applied to evaluate the surface-water quality of the Qingyi River within a BN model, achieving high accuracy [56].

The conditional probability is estimated using the following Equation (2):

$$P\left(X = x_i \middle| Pa\left(X\right) = pa_j\right) = \frac{Count\left(X = x_i,\ Pa(X) = pa_j\right)}{\sum_k Count\left(X = x_k, Pa(X) = pa_j\right)} \quad (2)$$

where X is the node (variable); x_i is the disconnected state of the node X; $Pa\ (X)$ represents parent node(s) of X; and pa_j denotes a combination of the states of parent nodes $Pa\ (X)$.

3.4. Assessment of Temporal Lag Effects

Supplementary analyses were conducted to evaluate whether static BN was a suitable method to explain the system dynamics. Cross-correlation analyses were performed between key hydrometeorological drivers and selected water quality parameters to identify potential lag-time response.

The lag analysis quantified the temporal dependencies between parameters, providing a basis for assessing whether the static BN assumption is justified.

3.5. Validation

To evaluate the BN model, the log-likelihood was used on the test dataset. This method is based on evaluating the joint probability of the observed test data using a trained BN model to obtain the log-likelihood score [57]. It was computed using Equation (3):

$$\mathcal{L} = \sum_{i=1}^{n} log\ P(x^{(i)}|model) \quad (3)$$

where $x^{(i)}$ is the observed value from the test dataset and $P(x^{(i)}|\text{model})$ is the probability of that value estimated by the BN model. This approach is suitable for evaluating the overall fit of a static BN, as it directly quantifies how well the model represents the joint distribution of all variables.

4. Results and Discussion

4.1. Parameter Learning Results

1. Air Temperature Influence on Water Temperature

The conditional probability analysis (Figure 4) showed a strong statistical dependence of water temperature on air temperature across different thermal regimes. During colder periods (<15 °C), approximately 96% of water temperature values were classified as low, indicating a pronounced thermal coupling between the atmosphere and the river. This relationship reflects reduced solar radiation and limited convective heat exchange, both of which constrain the energy transfer to the water column. Moderate air temperatures (15–25 °C) corresponded to only 72% moderate water temperatures, likely reflecting transitional seasonal variability, such as changes in solar radiation, cloud cover, and regional winds [58]. High air temperatures (>25 °C) produced mostly moderate water temperatures, highlighting the buffering effect of stable base flows in the Kiso River [59–61]. These patterns are consistent with prior studies showing that rivers with regulated or stable flows exhibit reduced thermal sensitivity to ambient air temperature changes.

2. Rainfall and River Flow Impact on Turbidity

Conditional probability analysis of turbidity (Figure 5) revealed that heavy rainfall combined with high river flow increased turbidity by approximately 80% probability of increased turbidity levels. This is consistent with sediment mobilization and particle resuspension processes that occur during high-energy hydrological events. Moderate rainfall induced variable turbidity responses, indicating non-linear interactions between precipitation, runoff, and sediment dynamics. Land-use changes near Nagoya City, such as the conversion of agricultural areas to urban infrastructure, further exacerbate sediment variability [62]. Such anthropogenic alterations enhance surface runoff and reduce infiltration, amplifying sediment delivery during rainfall events. Comparable findings were

observed in studies conducted in the Elbe River and semi-arid catchments of Spain, where intensified runoff during high-flow conditions resulted in sharp increases in suspended solids concentrations [63]. Such results highlight that variations in topography, soil disruption, and human-induced land-use modifications significantly influence the hydrological mechanisms governing turbidity formation and transport.

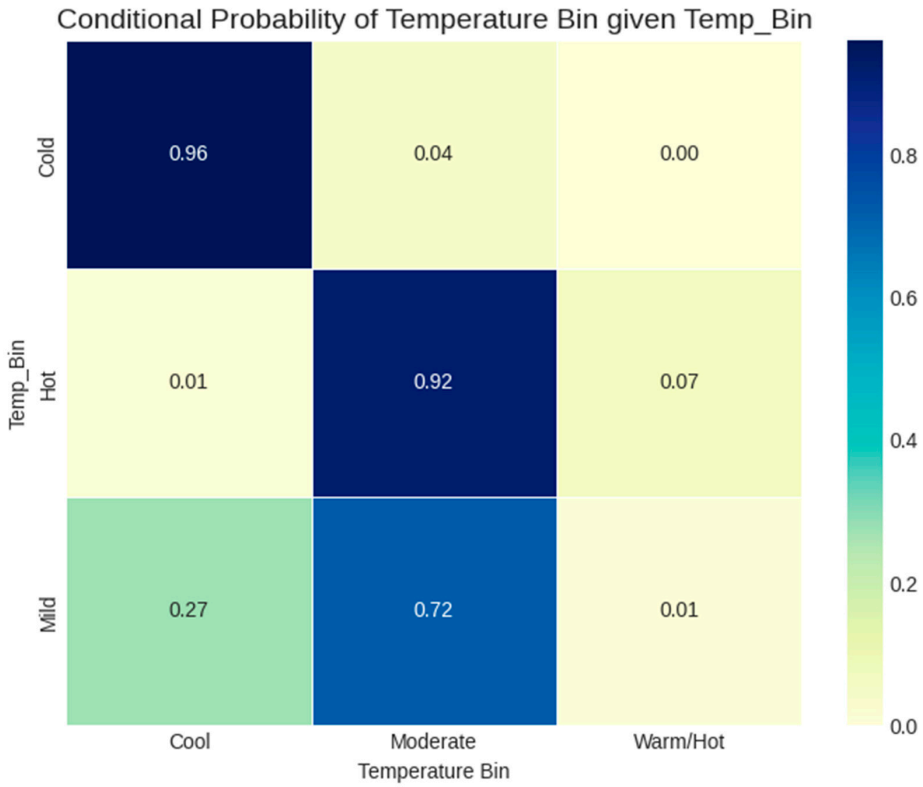


Figure 4. Conditional probability of water temperature.

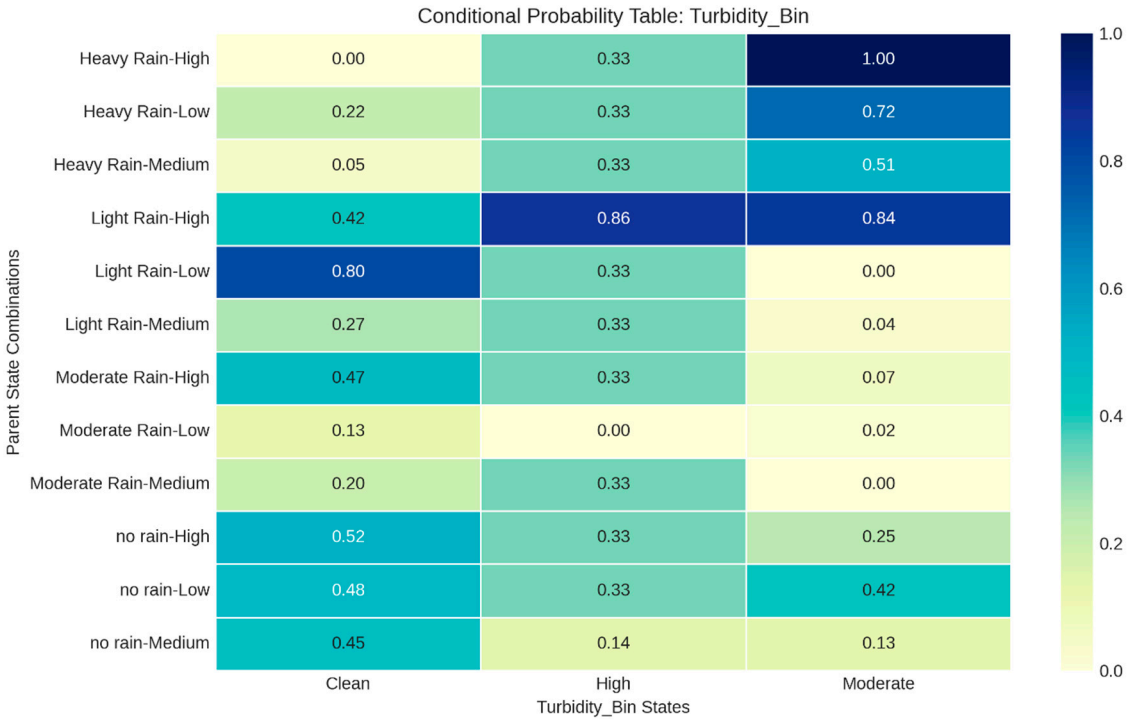


Figure 5. Conditional probability of turbidity.

3. Rainfall and Temperature Effects on Ammonia Levels

Ammonia concentrations exhibited a strong dependence on both rainfall and temperature regimes (Figure 6). Dry and warm conditions were associated with low ammonia levels, reflecting reduced surface runoff and enhanced nitrification efficiency under higher temperatures. Conversely, cool and wet periods led to elevated ammonia levels, primarily due to increased runoff transporting nitrogen-rich compounds from agricultural fields and urban surfaces into the river system [64,65]. Low temperatures further inhibited microbial nitrification processes, reducing the conversion of ammonia to nitrate and resulting in its accumulation within the water column [66]. Conditional probabilities also revealed a strong association between ammonia and organic pollution, reflecting that microbial decomposition of nitrogen-rich compounds contributes to particulate organic matter in the river. Deviations at moderate ammonia levels highlight the influence of discretization and environmental thresholds, demonstrating the limitations of binning strategies in probabilistic modeling.

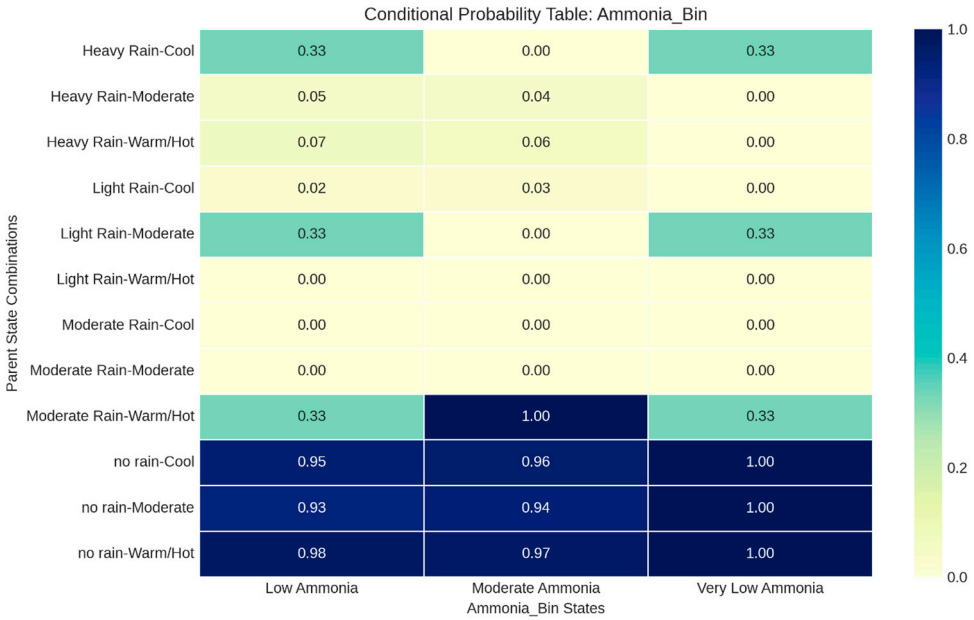


Figure 6. Conditional probability of Ammonia.

4. Dissolved Oxygen, Organic Pollution, and Temperature Influence on pH

The conditional probability analysis stresses the role of biological oxygen demand (BOD) and organic decomposition in determining pH values (Figure 7). The results revealed a neutral pH when DO was high and BOD was low, while moderate DO and increased BOD shifted the pH to acidic, neutral, and alkaline levels. These shifts in pH correlated with the release of organic acids during decomposition [67]. Temperature exerted a secondary but notable effect on pH. Warm water tends to lower gas solubility and alter ionization equilibria, leading to minor fluctuations in pH values [68]. These findings demonstrate the complex biochemical coupling between oxygen dynamics, organic matter decomposition, and acid–base balance in river systems.

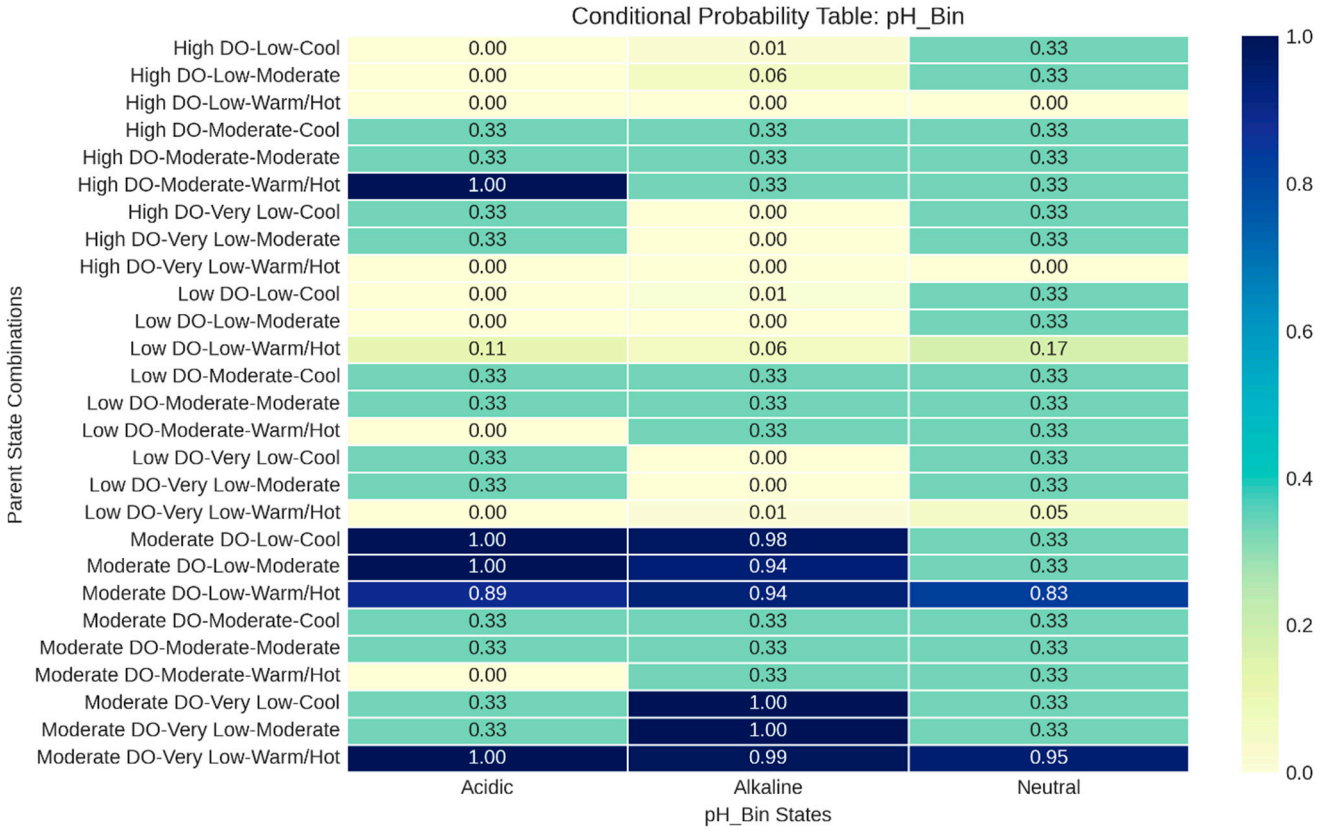


Figure 7. Conditional probability of pH.

5. Ammonia Contribution to Organic Pollution

A strong relationship was observed between ammonia and organic pollution, which is referred to as the total suspended solids (TSS), reflecting the concentration of particulate organic matter in the water, with very low ammonia levels (<0.005 mg/L) correlating with 97.7% of very low organic pollution (≤0.1 mg/L) (Figure 8). Ammonia was significantly impacted by the microbial decomposition of nitrogen-rich compounds. For instance, a case study of the Shitalakshya River in Bangladesh demonstrated the effect of organic matter decomposition on elevated ammonia levels during dry months, which further exacerbated the water quality [69]. However, A clear distinction in this pattern emerged when moderate (>0.02 mg/L) ammonia concentration was correlated with very low organic pollution. This change could be due to the lack of ammonia in the water and the influence of the national environmental standards discretization used for the model binning strategy.

6. River flow Effects on EC

This study modeled EC in the Kiso River as a function of river flow (Figure 9). During high-flow conditions, the analysis revealed a high probability (63%) for low EC values. This could be due to water diluting the dissolved ions concentration, leading to lower EC values [70]. The conditional probability indicated medium- and low-flow conditions, leading to a moderate EC. This was also explained by lower discharge, reduced dilution, and relatively increased EC levels. Lower river sections of the Kiso River reduce dilution, elevating EC levels as pollutants from varied land-uses become more concentrated. A study in the Kiso River Basin indicated high levels of dissolved ions near localized pollution sources, highlighting the impact of land-use when river flow is low, as reduced dilution increases pollutant impact [71].

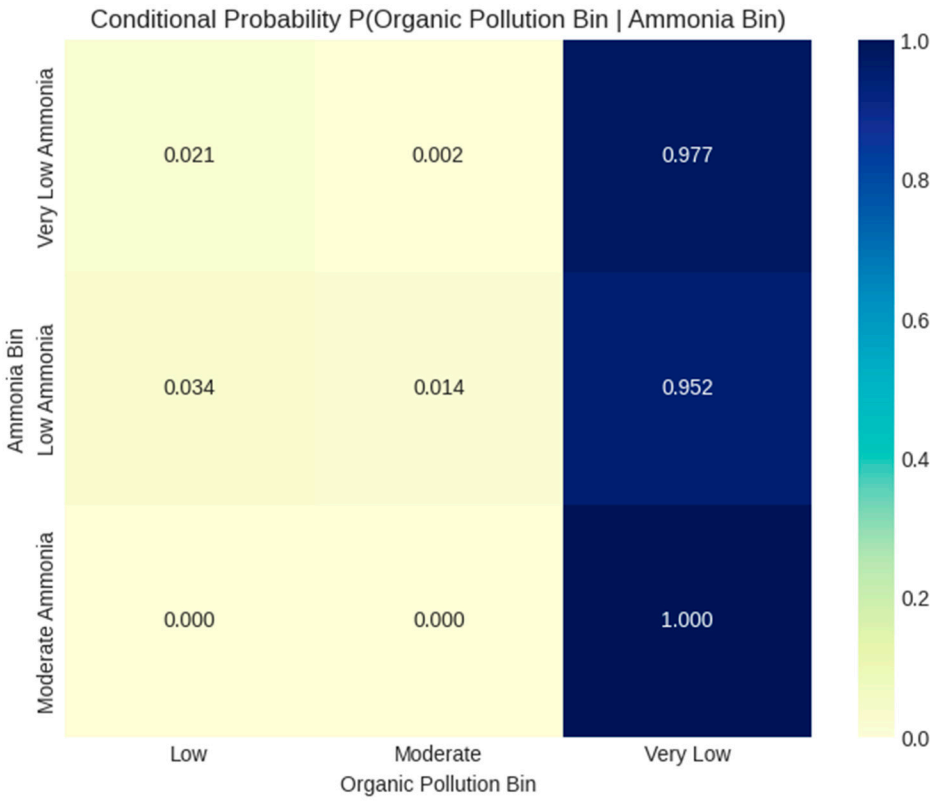


Figure 8. Conditional probability of organic pollution.

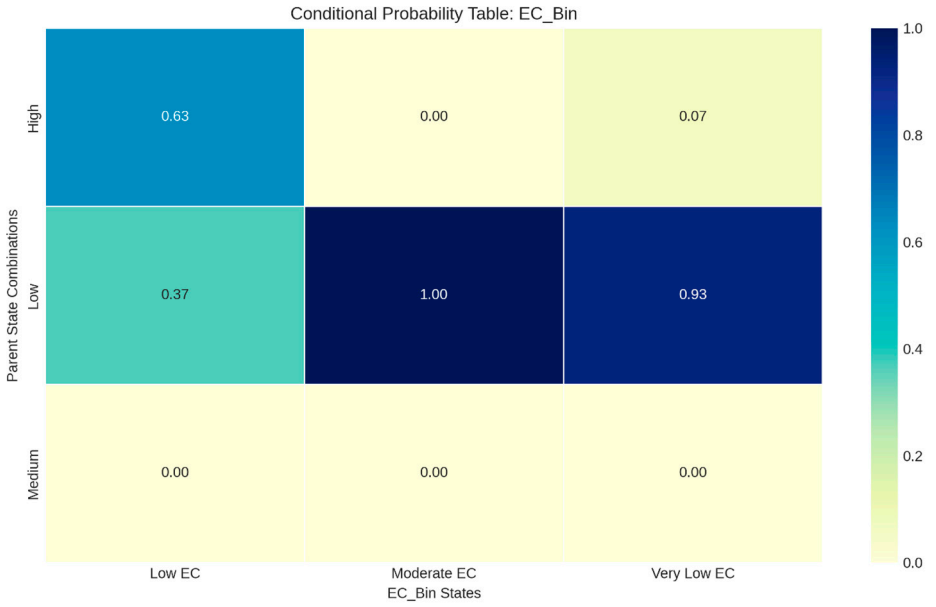


Figure 9. Conditional probability of electrical conductivity.

7. Influence of River Flow, Turbidity, and Temperature on Dissolved Oxygen

The conditional probability analysis (Figure 10) confirmed the interactive influence of river flow, turbidity, and temperature on DO concentrations. During high-flow periods, elevated turbidity and low water temperature coincided with higher DO levels, likely due to increased turbulence enhancing air–water gas exchange. Although turbidity reduces light penetration and thereby limits photosynthetic oxygen production, the physical re-aeration effect of strong water movement dominates under such conditions [72].

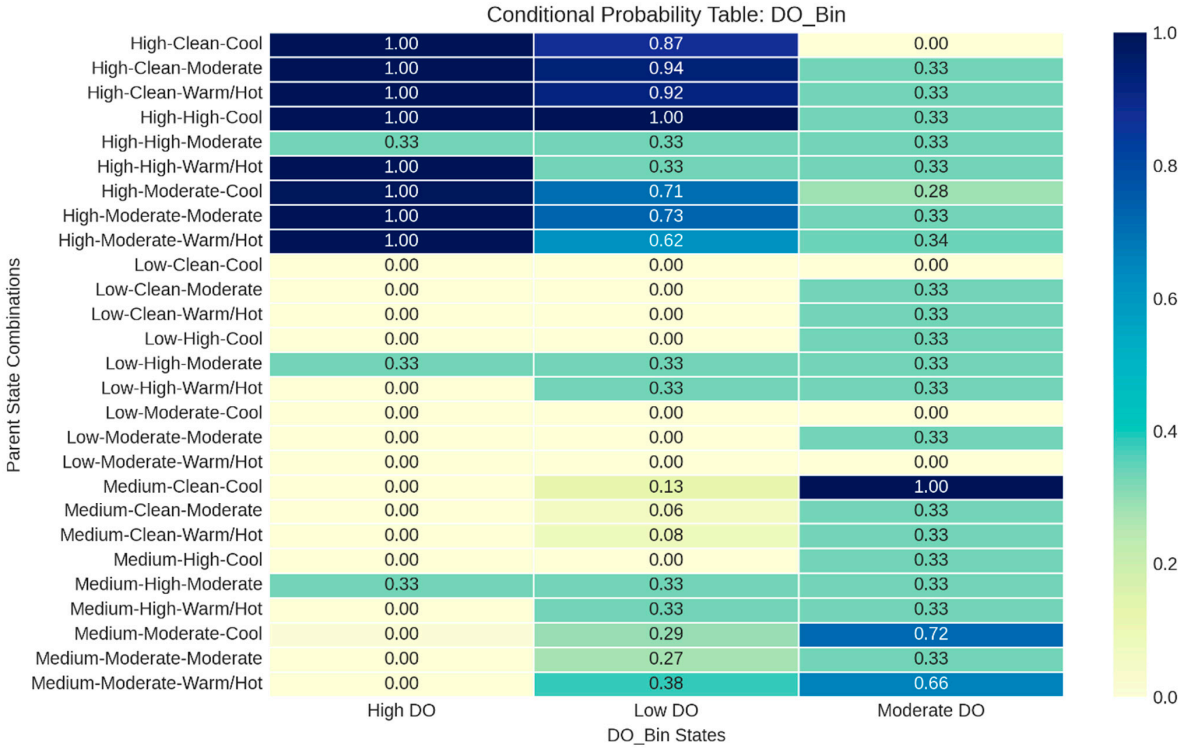
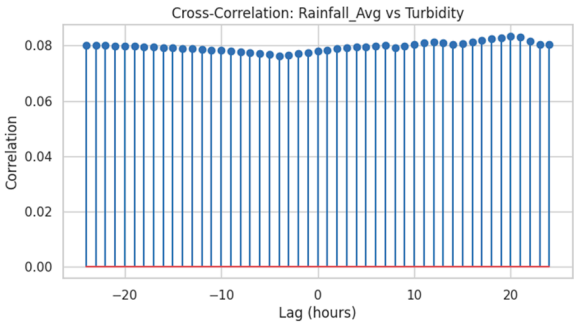


Figure 10. Conditional probability of dissolved oxygen.

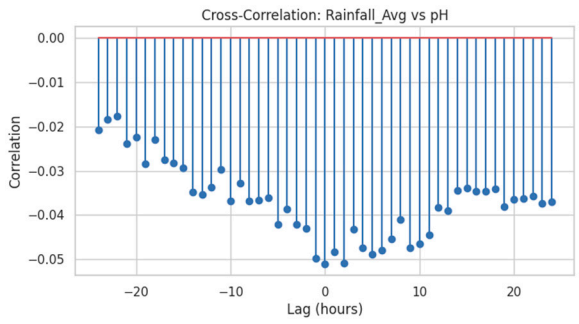
In contrast, moderate flow and elevated water temperature corresponded to lower DO concentrations, consistent with the inverse solubility of oxygen in warm water and enhanced biological oxygen consumption. These findings collectively illustrate the delicate balance between hydrodynamic conditions and biochemical processes governing oxygen availability in lotic systems.

4.2. Short-Term Responses and Lag Effects

The cross-correlation heatmaps (Figure 11a–u) presented detailed insights into the temporal dynamics between hydrometeorological drivers and water quality responses. Most parameters, including water temperature and dissolved oxygen, responded almost instantaneously to air temperature changes, reflecting rapid heat exchange and immediate oxygen solubility adjustments. Electrical conductivity and organic pollution similarly exhibited near-zero lag responses to meteorological drivers, confirming their short-term sensitivity to flow and atmospheric fluctuations.

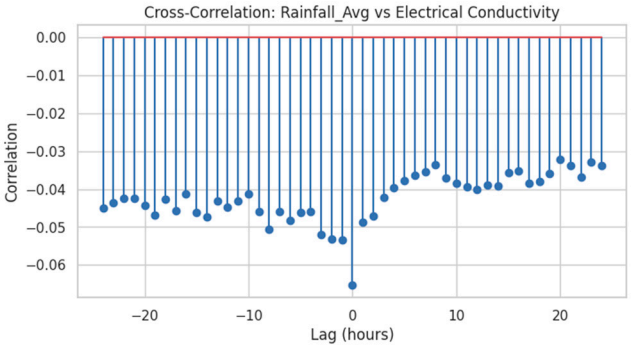


(**a**)

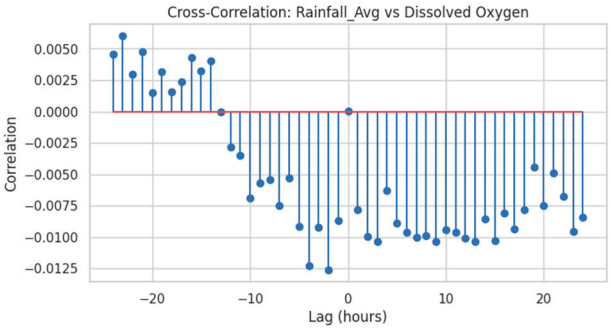


(**b**)

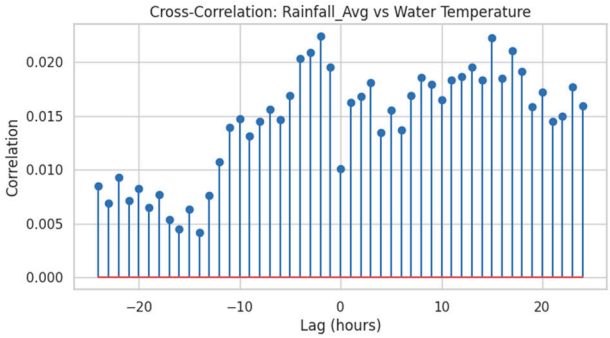
Figure 11. *Cont.*



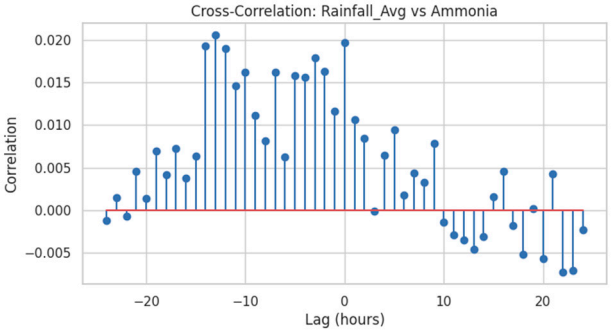
(**c**)



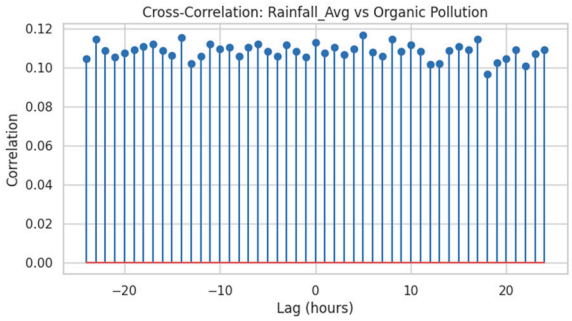
(**d**)



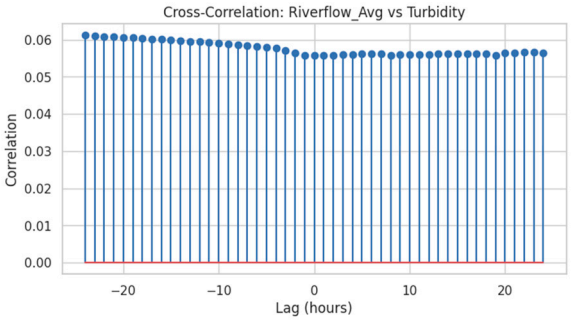
(**e**)



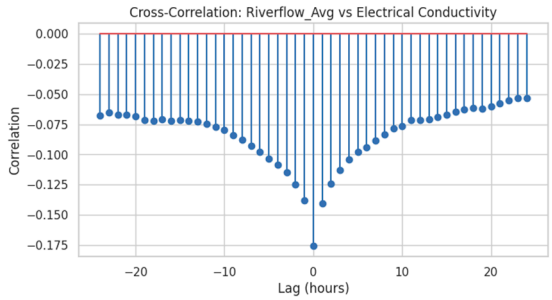
(**f**)



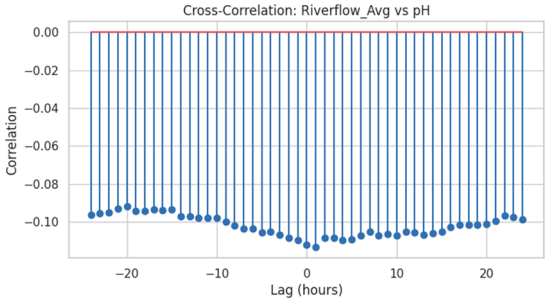
(**g**)



(**h**)

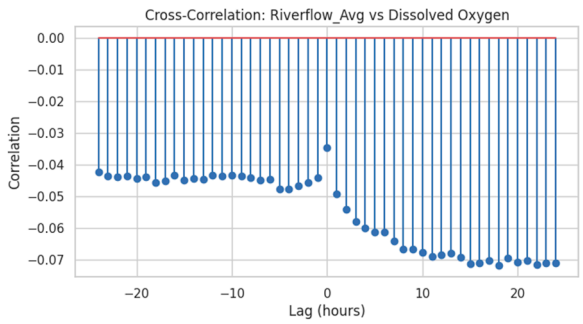


(**i**)

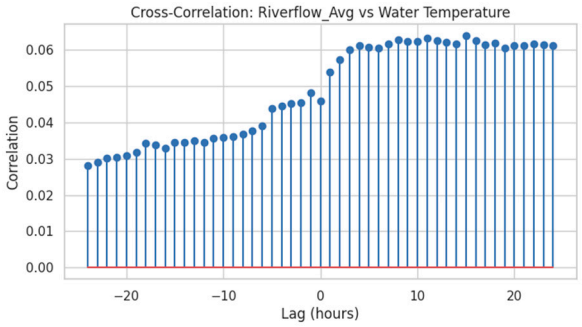


(**j**)

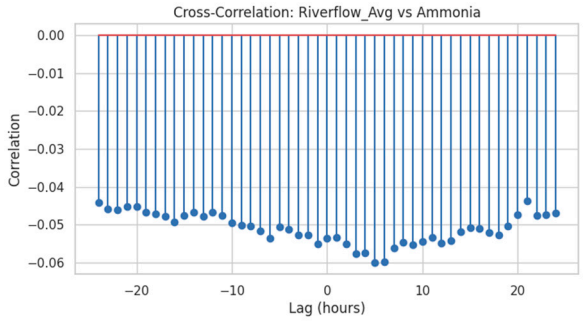
Figure 11. *Cont.*



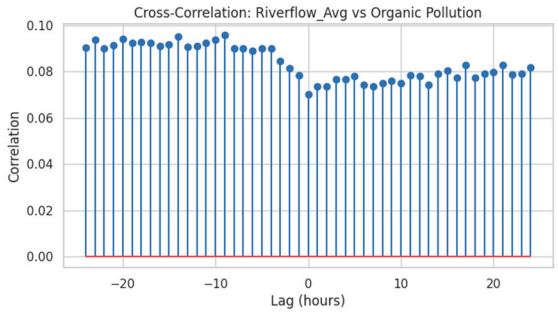
(**k**)



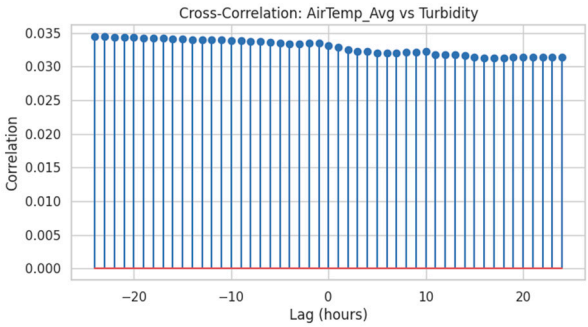
(**l**)



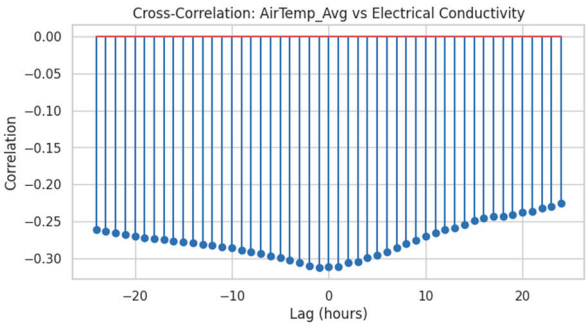
(**m**)



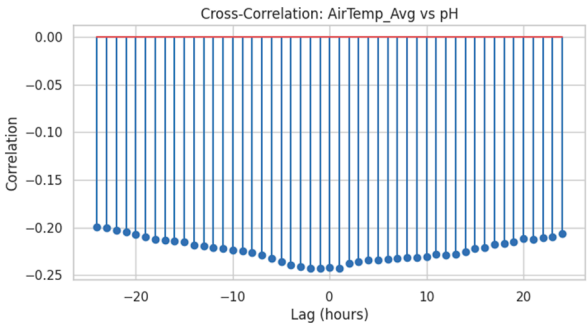
(**n**)



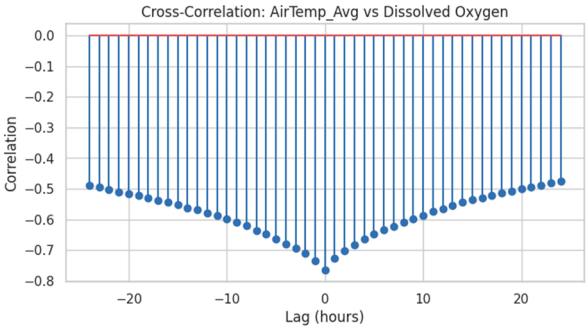
(**o**)



(**p**)

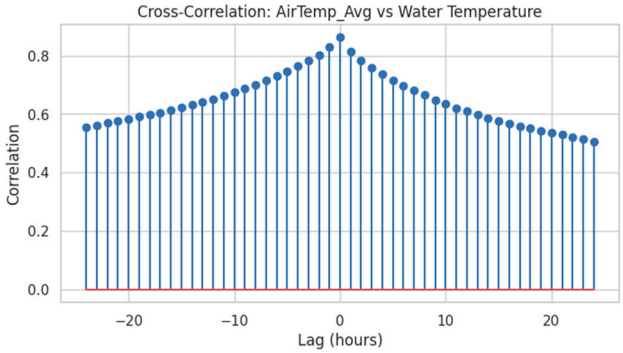


(**q**)

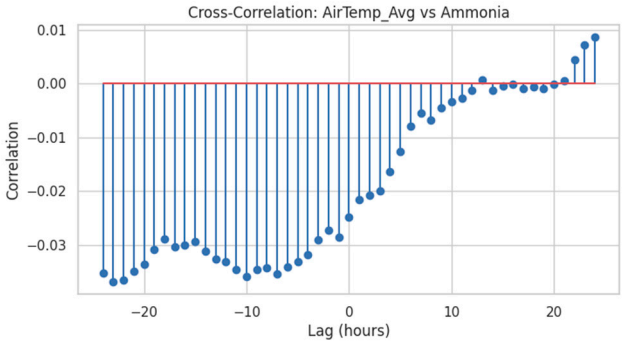


(**r**)

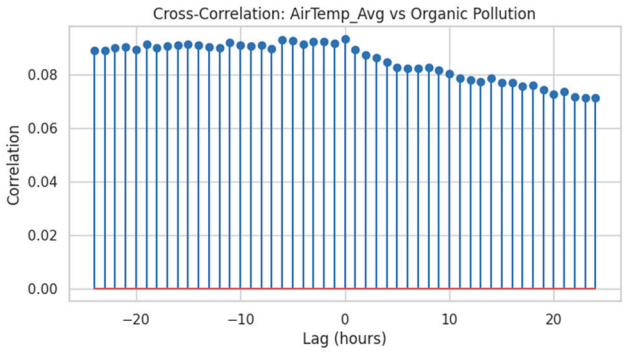
Figure 11. *Cont.*



(**s**)



(**t**)



(**u**)

Figure 11. (**a**) Cross-Correlation Heatmap: Rainfall_Avg vs. Turbidity. (**b**) Cross-Correlation Heatmap: Rainfall_Avg vs. pH. (**c**) Cross-Correlation Heatmap: Rainfall_Avg vs. Electrical Conductivity. (**d**) Cross-Correlation Heatmap: Rainfall_Avg vs. Dissolved Oxygen. (**e**) Cross-Correlation Heatmap: Rainfall_Avg vs. Water Temperature. (**f**) Cross-Correlation Heatmap: Rainfall_Avg vs. Ammonia. (**g**) Cross-Correlation Heatmap: Rainfall_Avg vs. Organic Pollution. (**h**) Cross-Correlation Heatmap: Riverflow_Avg vs. Turbidity. (**i**) Cross-Correlation Heatmap: Riverflow_Avg vs. Electrical Conductivity. (**j**) Cross-Correlation Heatmap: Riverflow_Avg vs. pH. (**k**) Cross-Correlation Heatmap: Riverflow_Avg vs. Dissolved Oxygen. (**l**) Cross-Correlation Heatmap: Riverflow_Avg vs. Water Temperature. (**m**) Cross-Correlation Heatmap: Riverflow_Avg vs. Ammonia. (**n**) Cross-Correlation Heatmap: Riverflow_Avg vs. Organic Pollution. (**o**) Cross-Correlation Heatmap: AirTemp_Avg vs. Turbidity. (**p**) Cross-Correlation Heatmap: AirTemp_Avg vs. Electrical Conductivity. (**q**) Cross-Correlation Heatmap: AirTemp_Avg vs. pH. (**r**) Cross-Correlation Heatmap: AirTemp_Avg vs. Dissolved Oxygen. (**t**) Cross-Correlation Heatmap: AirTemp_Avg vs. Ammonia. (**s**) Cross-Correlation Heatmap: AirTemp_Avg vs. Water Temperature. (**u**) Cross-Correlation Heatmap: AirTemp_Avg vs. Organic Pollution. Blue markers represent the cross-correlation coefficient at each time lag, and the red horizontal line indicates zero correlation as a reference baseline.

Overall, approximately 57% of the modeled water quality parameters showed immediate (0 h lag) responses, while an additional 29–43% exhibited short lags ($\leq$5 h) with weaker correlations, implying minimal delay in system response. Only turbidity displayed a significant lagged response (~20 h after rainfall), indicating the time required for runoff-induced sediment transport to reach the river channel.

These results suggest that a static Bayesian Network (BN) framework sufficiently captures the primary probabilistic dependencies within the Kiso River system. While a dynamic BN could represent delayed turbidity responses more explicitly, the marginal improvement in predictive accuracy does not justify the increased computational complexity. Thus, the static BN provides a parsimonious yet robust representation of short-term hydrometeorological–water quality interactions

4.3. Model Validation

The calculated log-likelihood of the held-out test data for the Bayesian Network was −60,689.45, averaging −4.62 per test instance. This indicates that the BN adequately captures the overall probabilistic dependencies among water quality parameters and hydrometeorological drivers. As the purpose of this evaluation is to assess the general fit of the static BN, the log-likelihood provides a reasonable and sufficient metric to demonstrate that the model reliably represents the joint distribution of the observed variables [73].

4.4. Recommendations and Policy Interventions

- Season-specific water temperature monitoring should be established during transitional seasons to overcome the variability in air temperature changes.
- Application of sustainable agriculture, reforestation, and robust land-use strategies is necessary to reduce sediment erosion during heavy precipitation events.
- Improving monitoring practices for ammonia and organic pollution during cold and wet conditions is warranted.
- Real-time water quality monitoring, such as IoT-based sensors, can be used for early detection of high levels of ammonia and changes in dissolved oxygen.

5. Conclusions

This study applied a discrete Bayesian Network (BN) framework to analyze the influence of climatic and hydrological drivers on water quality in the Kiso River Basin. The analysis revealed key causal relationships, including the effect of air temperature on water temperature and dissolved oxygen, the influence of river flow and rainfall on turbidity, and the interactions among ammonia, organic pollution, and other physicochemical parameters. High-frequency, seven-year monitoring data enabled a robust assessment of both immediate and short-lag responses, demonstrating that a static BN can adequately capture the primary probabilistic dependencies in the system.

The study's findings provide actionable insights for water quality management, such as the need for season-specific monitoring of water temperature, targeted management of sediment transport during heavy rainfall, and real-time tracking of ammonia and dissolved oxygen levels.

Limitations include discretization of continuous variables, assumptions of spatial stationarity, and the exclusion of land-use and point-source pollution data. Future work could integrate additional environmental indicators and apply complementary approaches, such as generalized additive models or machine learning methods, to improve predictive performance and causal inference.

Overall, the BN approach offers a scalable and interpretable framework for assessing water quality risks, supporting adaptive management under variable climatic and hydrological conditions, and informing evidence-based policy interventions in dynamic river systems.

Author Contributions: Conceptualization, O.M. and N.H.; methodology, O.M. and N.H.; formal analysis, O.M.; writing—original draft preparation, O.M.; writing—review and editing, O.M. and N.H.; visualization, O.M.; supervision, N.H. All authors have read and agreed to the published version of the manuscript.

Funding: This research was funded by the Environmental Research and Technology Development Fund (JPMEERF20S11816) of the Environmental Restoration and Conservation Agency of Japan.

Data Availability Statement: Meteorological data for air temperature presented in the study are openly available from the Japan Meteorological Agency (JMA) (www.data.jma.go.jp/). Similarly,

rainfall and river flow data are available from the Japan Ministry of Land, Infrastructure, Transport and Tourism Restrictions apply to the availability of water quality data.

Conflicts of Interest: The authors declare no conflict of interest.

References

1. Liu, C.; Hu, Y.; Sun, F.; Ma, L.; Wang, W.; Luo, B.; Wang, Y.; Zhang, H. Quantitative Analysis of the Driving Factors of Water Quality Variations in the Minjiang River in Southwestern China. *Water* **2023**, *15*, 3299. [CrossRef]
2. Mummidivarapu, S.K.; Rehana, S.; Rao, Y.R.S. Mapping and assessment of river water quality under varying hydro-climatic and pollution scenarios by integrating QUAL2K, GEFC, and GIS. *Environ. Res.* **2023**, *239*, 117250. [CrossRef]
3. Wan, L.; Wang, X.H.; Peirson, W. Impacts of Climate Change and Non-Point-Source Pollution on Water Quality and Algal Blooms in the Shoalhaven River Estuary, NSW, Australia. *Water* **2022**, *14*, 1914. [CrossRef]
4. Schaffer-Smith, D.; DeMeester, J.E.; Tong, D.; Myint, S.W.; Libera, D.A.; Muenich, R.L. Landscape Pollution Source Dynamics Highlight Priority Locations for Basin-Scale Interventions to Protect Water Quality Under Hydroclimatic Variability. *Earths Future* **2023**, *11*, e2022EF003137. [CrossRef]
5. Bastaraud, A.; Perthamei, E.; Rakotondramangai, J.M.; Mahazosaotra, J.; Ravaonindrina, N.; Jambouid, R. The impact of rainfall on drinking water quality in Antananarivo, Madagascar. *PLoS ONE* **2020**, *15*, e0218698. [CrossRef] [PubMed]
6. Ye, H.; Yang, D.; Zhang, T.; Zhang, X.; Ladochy, S.; Ellison, M. The Impact of Climatic Conditions on Seasonal River Discharges in Siberia. *J. Hydrometeorol.* **2004**, *5*, 286–295. [CrossRef]
7. Salila, E.; Sharma, M.P.; Singh, R. Climate Change Impacts on Water Quality of Water Bodies-A Review. *Int. J. Environ. Clim. Change* **2020**, *10*, 26–37. [CrossRef]
8. Surendra, P.; Saurabh, A.H. Impact Analysis of Urbanization and Industrialization on Water Quality of Vrishabhavathi River. *Geogr. Anal.* **2021**, *10*, 45–51. [CrossRef]
9. Yang, X.; Tan, L.; He, R.; Fu, G.; Ye, J.; Liu, Q.; Wang, G. Stochastic sensitivity analysis of nitrogen pollution to climate change in a river basin with complex pollution sources. *Environ. Sci. Pollut. Res.* **2017**, *24*, 26545–26561. [CrossRef]
10. Huang, J.; Huang, Y.; Zhang, Z. Coupled effects of natural and anthropogenic controls on seasonal and spatial variations of river water quality during baseflow in a coastal watershed of Southeast China. *PLoS ONE* **2014**, *9*, e91528. [CrossRef]
11. Saranathan, A.M.; Werther, M.; Balasubramanian, S.V.; Odermatt, D.; Pahlevan, N. Assessment of advanced neural networks for the dual estimation of water quality indicators and their uncertainties. *Front. Remote Sens.* **2024**, *5*, 1383147. [CrossRef]
12. Fonseca, A.; Botelho, C.; Boaventura, R.A.R.; Vilar, V.J.P. Evaluating the Effects of Parameter Uncertainty on River Water Quality Predictions. *Resources* **2024**, *13*, 106. [CrossRef]
13. Zhang, C.; Nong, X.; Behzadian, K.; Campos, L.C.; Chen, L.; Shao, D. A new framework for water quality forecasting coupling causal inference, time-frequency analysis and uncertainty quantification. *J. Environ. Manag.* **2024**, *350*, 119613. [CrossRef]
14. Roostaee, M.; Deng, Z. HSPF-based watershed-scale water quality modeling and uncertainty analysis. *Environ. Sci. Pollut. Res.* **2019**, *26*, 8971–8991. [CrossRef]
15. Chawishborwornworng, C.; Luanwuthi, S.; Umpuch, C.; Puchongkawarin, C. Bootstrap approach for quantifying the uncertainty in modeling of the water quality index using principal component analysis and artificial intelligence. *J. Saudi Soc. Agric. Sci.* **2024**, *23*, 17–33. [CrossRef]
16. Zheng, Y.; Han, F. Markov Chain Monte Carlo (MCMC) uncertainty analysis for watershed water quality modeling and management. *Stoch. Environ. Res. Risk Assess.* **2016**, *30*, 293–308. [CrossRef]
17. Yan, X.; Lu, W.; An, Y.; Chang, Z. Uncertainty analysis of parameters in non-point source pollution simulation: Case study of the application of the Soil and Water Assessment Tool model to Yitong River watershed in northeast China. *Water Environ. J.* **2019**, *33*, 390–400. [CrossRef]
18. Li, R.A.; McDonald, J.A.; Sathasivan, A.; Khan, S.J. A multivariate Bayesian network analysis of water quality factors influencing trihalomethanes formation in drinking water distribution systems. *Water Res.* **2021**, *190*, 116712. [CrossRef]
19. Wei, Z.; Alam, S.; Verma, M.; Hilderbran, M.; Wu, Y.; Anderson, B.; Ho, D.E.; Suckale, J. Integrating water quality data with a Bayesian network model to improve spatial and temporal phosphorus attribution: Application to the Maumee River Basin. *J. Environ. Manag.* **2024**, *360*, 121120. [CrossRef]
20. Vogel, K.; Riggelsen, C.; Korup, O.; Scherbaum, F. Bayesian network learning for natural hazard analyses. *Nat. Hazards Earth Syst. Sci.* **2014**, *14*, 2605–2626. [CrossRef]
21. Scutari, M. Bayesian network models for incomplete and dynamic data. *Stat. Neerl.* **2020**, *74*, 397–419. [CrossRef]
22. Krapu, C.; Stewart, R.; Rose, A. A Review of Bayesian Networks for Spatial Data. *ACM Trans. Spat. Algorithms Syst.* **2023**, *9*, 1–21. [CrossRef]
23. Govender, I.H.; Sahlin, U.; O'Brien, G.C. Bayesian Network Applications for Sustainable Holistic Water Resources Management: Modeling Opportunities for South Africa. *Risk Anal.* **2022**, *42*, 1346–1364. [CrossRef] [PubMed]

24. Marcot, B.G.; Penman, T.D. Advances in Bayesian network modelling: Integration of modelling technologies. *Environ. Model. Softw.* **2019**, *111*, 386–393. [CrossRef]
25. Adams, K.J.; Macleod, C.A.J.; Metzger, M.J.; Melville, N.; Helliwell, R.C.; Pritchard, J.; Glendell, M. Developing a Bayesian network model for understanding river catchment resilience under future change scenarios. *Hydrol. Earth Syst. Sci.* **2023**, *27*, 2205–2225. [CrossRef]
26. Phan, T.D.; Smart, J.C.R.; Stewart-Koster, B.; Sahin, O.; Hadwen, W.L.; Dinh, L.T.; Tahmasbian, I.; Capon, S.J. Applications of bayesian networks as decision support tools for water resource management under climate change and socio-economic stressors: A critical appraisal. *Water* **2019**, *11*, 2642. [CrossRef]
27. Phan, T.D.; Sahin, O.; Smart, J.C.R. System Dynamics and Bayesian Network Models for Vulnerability and Adaptation Assessment of a Coastal Water Supply and Demand System. In Proceedings of the 8th International Congress on Environmental Modelling and Software (iEMSs 2016), Session D8: Innovative, Participatory and Integrated Modelling for Climate Change Assessments and Management, Toulouse, France, 11 July 2016. Available from BYU ScholarsArchive.
28. Phan, T.D.; Smart, J.C.R.; Capon, S.J.; Hadwen, W.L.; Sahin, O. Applications of Bayesian belief networks in water resource management: A systematic review. *Environ. Model. Softw.* **2016**, *85*, 98–111. [CrossRef]
29. Aguilera, P.A.; Fernández, A.; Fernández, R.; Rumí, R.; Salmerón, A. Bayesian networks in environmental modelling. *Environ. Model. Softw.* **2011**, *26*, 1376–1388. [CrossRef]
30. Kaikkonen, L.; Parviainen, T.; Rahikainen, M.; Uusitalo, L.; Lehikoinen, A. Bayesian Networks in Environmental Risk Assessment: A Review. *Integr. Environ. Assess. Manag.* **2021**, *17*, 62–78. [CrossRef]
31. Shi, P.; Yang, T.; Yong, B.; Xu, C.-Y.; Li, Z.; Wang, X.; Qin, Y.; Zhou, X. Some statistical inferences of parameter in MCMC approach and the application in uncertainty analysis of hydrological simulation. *J. Hydrol.* **2023**, *617*, 128767. [CrossRef]
32. Jeremiah, E.; Sisson, S.; Marshall, L.; Mehrotra, R.; Sharma, A. Bayesian calibration and uncertainty analysis of hydrological models: A comparison of adaptive Metropolis and sequential Monte Carlo samplers. *Water Resour. Res.* **2011**, *47*, W07547. [CrossRef]
33. Camacho, R.A.; Martin, J.L.; McAnally, W.; Díaz-Ramirez, J.; Rodriguez, H.; Sucsy, P.; Zhang, S. A Comparison of Bayesian Methods for Uncertainty Analysis in Hydraulic and Hydrodynamic Modeling. *J. Am. Water Resour. Assoc.* **2015**, *51*, 1372–1393. [CrossRef]
34. Arhonditsis, G.B.; Perhar, G.; Zhang, W.; Massos, E.; Shi, M.; Das, A. Addressing equifinality and uncertainty in eutrophication models. *Water Resour. Res.* **2008**, *44*, W01420. [CrossRef]
35. Tan, J.; Cao, J.; Cui, Y.; Duan, Q.; Gong, W. Comparison of the generalized likelihood uncertainty estimation and markov chain monte carlo methods for uncertainty analysis of the oryza_v3 model. *Agron. J.* **2019**, *111*, 555–564. [CrossRef]
36. Sun, X.Y.; Newham, L.T.H.; Croke, B.F.W.; Norton, J.P. Three complementary methods for sensitivity analysis of a water quality model. *Environ. Model. Softw.* **2012**, *37*, 19–29. [CrossRef]
37. Hirsch, R.M.; Archfield, S.A.; De Cicco, L.A. A bootstrap method for estimating uncertainty of water quality trends. *Environ. Model. Softw.* **2015**, *73*, 148–166. [CrossRef]
38. Allawi, M.F.; Salih, S.Q.; Kassim, M.; Ramal, M.M.; Mohammed, A.S.; Yaseen, Z.M. Application of Computational Model Based Probabilistic Neural Network for Surface Water Quality Prediction. *Mathematics* **2022**, *10*, 3960. [CrossRef]
39. Zhang, X.; Zhao, K. Bayesian Neural Networks for Uncertainty Analysis of Hydrologic Modeling: A Comparison of Two Schemes. *Water Resour. Manag.* **2012**, *26*, 2365–2382. [CrossRef]
40. Shrestha, S.; Kazama, F. Assessment of surface water quality using multivariate statistical techniques: A case study of the Fuji river basin, Japan. *Environ. Model. Softw.* **2007**, *22*, 464–475. [CrossRef]
41. Ren, J.Y.; Liu, H.M.; Ding, S.Y.; Cao, Z.H. Spatio-Temporal Variation Characteristics of Water Quality and Its Response to Climate: A Case Study in Yihe River Basin. *J. Environ. Inform. Lett.* **2021**, *6*, 10–22. [CrossRef]
42. Coletti, C.; Testezlaf, R.; Ribeiro, T.A.P.; De Souza, R.T.G.; Pereira, D.D.A. Water quality index using multivariate factorial analysis. *Rev. Bras. Eng. Agricola Ambient.* **2010**, *14*, 517–522. [CrossRef]
43. Ankan, A.; Textor, J. pgmpy: A Python Toolkit for Bayesian Networks. *J. Mach. Learn. Res.* **2024**, *25*, 1–8.
44. Ministry of the Environment, Japan. Environmental Quality Standards for Water Pollution. n.d. Available online: https://www.env.go.jp/kijun/index.html (accessed on 30 June 2025).
45. Beuzen, T.; Marshall, L.; Splinter, K.D. A comparison of methods for discretizing continuous variables in Bayesian Networks. *Environ. Model. Softw.* **2018**, *108*, 61–66. [CrossRef]
46. Blåfield, L.; Marttila, H.; Kasvi, E.; Alho, P. Temporal shift of hydroclimatic regime and its influence on migration of a high latitude meandering river. *J. Hydrol.* **2024**, *633*, 130935. [CrossRef]
47. Srinivas, R.; Singh, A.P.; Dhadse, K.; Magner, J. Hydroclimatic river discharge and seasonal trends assessment model using an advanced spatio-temporal model. *Stoch. Environ. Res. Risk Assess.* **2020**, *34*, 381–396. [CrossRef]
48. Bolade, O.; Hansen, A.T. Inferring drivers of nitrate and sediment event dynamics from hysteresis metrics for two large agricultural watersheds. *Hydrol. Process.* **2023**, *37*, e14969. [CrossRef]

49. Xiao, Y.; Zhang, C.; Zhang, T.; Luan, B.; Liu, J.; Zhou, Q.; Li, C.; Cheng, H. Transport processes of dissolved and particulate nitrogen and phosphorus over urban road surface during rainfall runoff. *Sci. Total Environ.* **2024**, *948*, 174905. [CrossRef]
50. Huang, X.; Zhu, Y.; Lin, H.; She, D.; Li, P.; Lang, M.; Xia, Y. High-frequency monitoring during rainstorm events reveals nitrogen sources and transport in a rural catchment. *J. Environ. Manag.* **2024**, *362*, 121308. [CrossRef]
51. Hu, J.; Ouyang, W.; Yang, Z. Impacts of extreme climate on nitrogen loss in different forms and pollution risk with the copula model. *J. Hydrol.* **2023**, *620*, 129412. [CrossRef]
52. Wu, L.; Han, C.; Zhu, G.; Zhong, W.; Atomi, H. Responses of Active Ammonia Oxidizers and Nitrification Activity in Eutrophic Lake Sediments to Nitrogen and Temperature. *Appl. Environ. Microbiol.* **2019**, *85*, e00258-19. [CrossRef]
53. Camargo, J.A.; Alonso, Á. Ecological and toxicological effects of inorganic nitrogen pollution in aquatic ecosystems: A global assessment. *Environ. Int.* **2006**, *32*, 831–849. [CrossRef]
54. Nunes, P.; Roland, F.; Amado, A.M.; Resende Nda, S.; Cardoso, S.J. Responses of Phytoplanktonic Chlorophyll-a Composition to Inorganic Turbidity Caused by Mine Tailings. *Front. Environ. Sci.* **2022**, *9*, 605838. [CrossRef]
55. Zhang, J.; Yue, K.; Liu, W. *Learning and Inferences of the Bayesian Network with Maximum Likelihood Parameters*; Springer: Berlin/Heidelberg, Germany, 2008.
56. Xie, X.; Liu, Y.; Luo, Y.; Du, Q. Surface Water Quality Evaluation Based on Bayesian Network. *J. Coast. Res.* **2019**, *93*, 54–60. [CrossRef]
57. Reijnen, C.; Gogou, E.; Visser, N.C.M.; Engerud, H.; Ramjith, J.; van der Putten, L.J.M.; van de Vijver, K.; Santacana, M.; Bronsert, P.; Bulten, J.; et al. Preoperative risk stratification in endometrial cancer (ENDORISK) by a Bayesian network model: A development and validation study. *PLoS Med.* **2020**, *17*, e1003111. [CrossRef] [PubMed]
58. Tamiya, H. Four Seasons for Japan. In Proceedings of the General Meeting of the Association of Japanese Geographers; The Association of Japanese Geographers: Bunkyō, Japan, 2014; p. 67. [CrossRef]
59. Takeda, M.; Kimura, I.; Matsuo, N.; Yamazaki, Y.; Fujita, A. Study on water temperature change and its numerical simulation model in kiso river Wando. *Proc. Hydraul. Eng.* **2002**, *46*, 1097–1102. [CrossRef]
60. Kaandorp, V.P.; Doornenbal, P.J.; Kooi, H.; Peter Broers, H.; de Louw, P.G.B. Temperature buffering by groundwater in ecologically valuable lowland streams under current and future climate conditions. *J. Hydrol. X* **2019**, *3*, 100031. [CrossRef]
61. Onitsuka, K.; Yano, M.; Akiyama, J.; Nezu, I. Groundwater between adjacent rivers: Groundwater between Kiso and Nagara Rivers. *J. Appl. Mech.* **2004**, *7*, 929–936. [CrossRef]
62. Shirai, Y. Urbanization and land readjustment on the case of the lower basin of the Kiso river. *Geogr. Rev. Jpn.* **1967**, *40*, 66–86. [CrossRef]
63. Rodríguez-Blanco, M.L.; Taboada-Castro, M.M.; Taboada-Castro, M.T. Suspended sediment dynamics during a period of consecutive explosive cyclogeneses in rural temperate catchments: A case study from small-sized catchments in NW Spain. *Catena* **2020**, *187*, 104316. [CrossRef]
64. Wang, Y.; Dai, Q.; Ding, P.; Li, K.; Yi, X.; He, J.; Peng, X.; Yan, Y.; Zhao, M.; Yang, Y. Rapid Response of Runoff Carrying Nitrogen Loss to Extreme Rainfall in Gentle Slope Farmland in the Karst Area of SW China. *Water* **2022**, *14*, 3341. [CrossRef]
65. Liu, J.; Li, T.; He, B.; Xi, P. Effects of quantitative fertilization and straw mulch on runoff nitrate- and ammonium-nitrogen losses under natural rainfall events in purple soil sloping croplands, Southwest China. *Ecol. Eng.* **2024**, *201*, 107196. [CrossRef]
66. Berounsky, V.M.; Nixon, S.W. Temperature and annual cycle of nitrification in waters of Narragansett Bay. *Limnol. Ocean.* **1990**, *35*, 1610–1617. [CrossRef]
67. Ylla, I.; Romaní, A.M.; Sabater, S. Labile and Recalcitrant Organic Matter Utilization by River Biofilm Under Increasing Water Temperature. *Microb. Ecol.* **2012**, *64*, 593–604. [CrossRef] [PubMed]
68. Arango, C.P.; Beaulieu, J.J.; Fritz, K.M.; Hill, B.H.; Elonen, C.M.; Pennino, M.J.; Mayer, P.M.; Kaushal, S.S.; Balz, A.D. Urban infrastructure influences dissolved organic matter quality and bacterial metabolism in an urban stream network. *Freshw. Biol.* **2017**, *62*, 1917–1928. [CrossRef]
69. Md Serajuddin, M.d.S.; Chowdhury, M.d.A.I.; Haque, M.d.M.; Khan, T.A. The Concentration of Organic & Ammonium Pollution and their Relationship in River Water: A Case Study. *Sch. J. Eng. Technol.* **2024**, *12*, 82–88. [CrossRef]
70. Kurunc, A.; Yurekli, K.; Ozturk, F. Effect of Discharge Fluctuation on Water Quality Variables from the Yeşilırmak River. *Tarım Bilim. Derg.* **2005**, *11*, 189–195. [CrossRef]
71. Mano, H.; Iwasaki, Y.; Shinohara, N. Effect-based water quality assessment of rivers receiving discharges from legacy mines by using acute and chronic bioassays with two cladoceran species. *Water Supply* **2022**, *22*, 3603–3616. [CrossRef]

72. Wei, W.; Han, Y.; Zhou, Y. Nutrients and sea surface temperature drive harmful algal blooms in China's coastal waters over the past decades. *Environ. Res. Lett.* **2023**, *18*, 094068. [CrossRef]
73. Ye, B.; Shu, H.; Cao, M.; Zeng, F.; Qiu, G.; Dong, J.; Zhang, W.; Shan, J. A Bayesian network method for quantitative evaluation of defects in multilayered structures from Eddy current NDT signals. *Math. Probl. Eng.* **2014**, *2014*, 405707. [CrossRef]

Disclaimer/Publisher's Note: The statements, opinions and data contained in all publications are solely those of the individual author(s) and contributor(s) and not of MDPI and/or the editor(s). MDPI and/or the editor(s) disclaim responsibility for any injury to people or property resulting from any ideas, methods, instructions or products referred to in the content.